

ELECTRIC EQUIVALENT CIRCUIT FOR THE THICKENED EDGE LOAD SOLUTION IN A BULK ACOUSTIC WAVE RESONATOR

J. Verdú, P. de Paco, and Ó. Menéndez

Universitat Autònoma de Barcelona (UAB)
Q-Building, Campus of UAB
08193 Bellaterra (Cerdanyola del Vallès), Barcelona, Spain

Abstract—With the aim to improve the performance of Bulk Acoustic Wave resonators, the thickened edge load can be included on the top electrode. Using this solution, the energy trapping concept is forced, and lateral unwanted resonances are not present in the electrical behavior of the resonator. The way to design such a thickened edge load entails, on one hand, the presence of a resonant mode given by the thickened edge load; on the other hand, the degradation of the electromechanical coupling coefficient of the main thickness mode. In order to study the previous phenomena, the electric equivalent circuit has been developed. The obtained results have been validated with the three-dimensional simulations and compared with manufactured resonators.

1. INTRODUCTION

The actual communication systems demand devices with very high performance, small size and compatibility with the standard integrated circuits (IC) technologies. Devices based on bulk acoustic wave (BAW) resonators fulfill those requirements. However, the presence of spurious modes in the electrical behavior of BAW resonator requires some optimization techniques in order to minimize or avoid such unwanted modes. RF Filters are mainly affected by the presence of the unwanted modes, which appears as a ripple in the transmission passband [1]

The conventional BAW resonator presents a structure where, at the interface between the electroded and non-electroded regions, the boundary condition requires the presence of a thickness shear mode in the non-electroded region. In this case, the energy trapping

Corresponding author: J. Verdú (jordi.verdu@uab.es).

concept is not accomplished, leading to some of the trapped energy leaking away [2–4]. In order to avoid or minimize the unwanted resonances, some techniques have been applied to the BAW resonator design. On one hand, some works propose irregular shapes or non-parallel edges, which is called apodization, at the top electrode [5–8]. Using these techniques, the resonant path becomes much larger, which produces an attenuation of the unwanted mode. In spite of such attenuation, the presence of the unwanted mode is not avoided. On the other hand, as proposed in [9–11], the top electrode can be loaded with a thickened edge to force different regions with its respective characteristic propagation and mass loading condition as shown in Figure 1, necessary for the energy trapping concept. Unlike the previous techniques, in this case, unwanted lateral modes are not generated, achieving an improved performance in the electrical behavior of the BAW resonator.

The presence of the thickened edge load makes the available one-dimensional model not accurate enough, and thus three-dimensional simulations are required. However, as we propose in this work, every part of the structure under different mechanical conditions can be separately modeled in order to obtain the equivalent one-dimensional model for the proposed solution. Therefore, the computation time to obtain the electrical behavior of the BAW resonator is notably reduced with respect to the three-dimensional simulation. Thus, taking advantage of the analysis of the input electrical impedance for the resulting equivalent circuit, side effects coming from this solution will be analyzed and widely discussed. In order to validate the proposed equivalent circuit, the results have been compared against the three-dimensional simulation using the finite element method and also compared with manufactured resonators. Finally, the conclusions of the work will be presented.

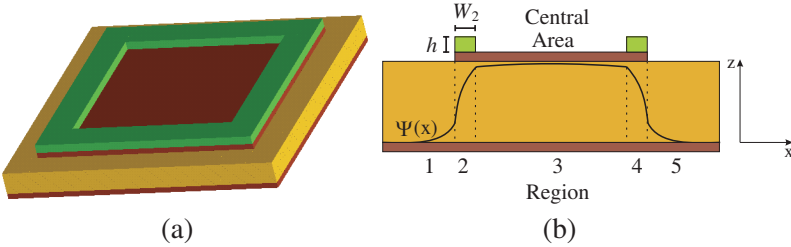


Figure 1. (a) Three-Dimensional view of a BAW resonator with the thickened edge load. (b) BAW resonator two-dimensional section with the mechanical distribution.

2. THICKENED EDGE LOAD SOLUTION

When the lateral dimensions are assumed to be finite in a BAW resonator, lateral acoustic waves, also known as Lamb waves, are also excited, and they cannot be predicted by means of one-dimensional models. Lamb waves have the particularity of being dispersive for a given ratio between the thickness and the lateral dimensions of the structure [12].

In Figure 1(a), the three-dimensional view of the BAW resonator is shown in which the thickened edge load has been included. The two-dimensional cross section in Figure 1(b) shows five different regions where different characteristic propagations and mass loading conditions are given. Due to the symmetry of the structure in the x -direction, Regions 1 and 5 and 2 and 4 are assumed to be equal since the mechanical and electrical conditions are the same. The mechanical displacement distribution for each Region r can be written as,

$$\Psi_r(x_r) = A_r e^{-jk_r x_r} + B_r e^{jk_r x_r} \quad (1)$$

where k_r is the wave number at the Region r . In order to analyze the propagation of the Lamb wave, the boundary conditions at the interfaces between regions must be stated. In this case, continuity of the mechanical displacement and equal stress on both sides of the interface are required. The boundary conditions can be expressed as,

$$\begin{aligned} \Psi_r(x_r = W_r) &= \Psi_{r+1}(x_{r+1} = 0) \\ \left. \frac{d\Psi_r}{dx} \right|_{x_r=W_r} &= \left. \frac{d\Psi_{r+1}}{dx} \right|_{x_{r+1}=0} \end{aligned} \quad (2)$$

where W_r corresponds to the width at Region r . In order to avoid unwanted resonances in the central area, that is Region 3, the mechanical displacement must be uniform and flat for the strongest resonant mode. This mode, known as a piston mode, is achieved when the derivative of the mechanical displacement at this frequency is zero, that is $\nabla\Psi = 0$. Applying the boundary conditions and the condition for the piston mode, the width W_2 for the thickened edge load can be obtained [9],

$$W_2 = \frac{\arctan \frac{K_1}{k_2} + n\pi}{k_2}, \quad n = 0, 1, \dots, N \quad (3)$$

where $k_1 = jK_1$ is the wave number at Region 1, K_1 a real number, and k_2 the wave number at Region 2. The width presents a periodical solution with n due to the periodicity of the trigonometrical functions.

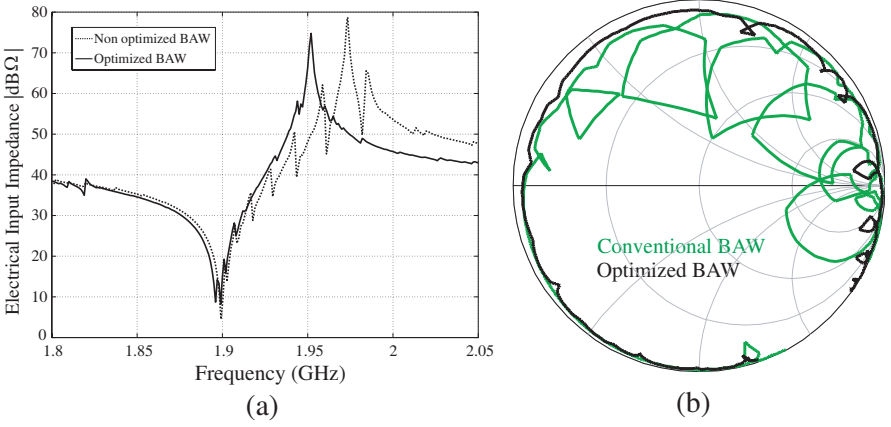


Figure 2. (a) Three-dimensional simulation for a conventional BAW resonator (dot line) and an improved BAW resonator with the thickened edge load (solid line). (b) Smith Chart representation.

In Figure 2(a), the comparison of the electrical impedance between a conventional BAW resonator and a thickened edge loaded BAW is shown. The thickened edge load has been designed using $h = 300$ nm and $n = 10$, leading to a width $W_2 = 11.65$ μm , where the piezoelectric material is ZnO, and the metal electrodes are made of aluminum. The used material properties for the ZnO are $c_{11} = 210$, $c_{12} = 121$, $c_{13} = 105$, $c_{33} = 211$, $c_{44} = 43$ [GN/m²]; $e_{15} = -0.48$, $e_{31} = -0.57$, $e_{33} = 1.32$ [C/m²]; $\varepsilon_{11} = 8.6$, $\varepsilon_{22} = 8.6$, $\varepsilon_{33} = 10$, where $[c]$ corresponds to the stiffness, $[e]$ the piezoelectric and $[\varepsilon]$ the permittivity matrix. The density has been set to $\rho = 5680$ [13]. In the case of the aluminum, the Young modulus has been set to $E = 63.61$ GPa, shear moduli to $G = 28.5$ GPa and Poisson's ratio $\sigma = 0.362$.

It can be seen that using the thickened edge load solution, the presence of unwanted modes between resonant frequencies is avoided. However, the position of the antiresonance frequency has been shifted to lower frequencies. This situation will be discussed in the following sections. On the other hand, the Smith Chart representation is shown in Figure 2(b). Each of the loops contained in the electrical response are due to the presence of spurious modes, where as expected, they are almost negligible in the optimized BAW resonator. Also note that the radio of the main loop in the optimized BAW resonator is higher than the conventional case, which is related with the quality factor Q . In the optimized BAW resonator, there is no energy leaking to the spurious modes, which makes the Q -value higher.

3. EQUIVALENT ELECTRIC CIRCUIT FOR THE THICKENED EDGE LOAD SOLUTION

The fundamental mode operation of the BAW resonator can be modeled by means of the Butterworth-Van Dyke (BVD) equivalent circuit considering infinitesimal electrodes. This circuit consists of a static capacitance C_0 , which is the parallel plate capacitor, in shunt configuration with a series L - C circuit corresponding to the motional arm [14]. However, when the thickened edge load is included, two different regions must be distinguished in which the mass loading conditions are different, so, the application of the one-dimensional BVD equivalent circuit to model the full structure is not a valid approach.

The mass loading effect is the group of effects related with the metal electrodes deposition that appears in the electrical behavior of the BAW resonator. The design parameter that is mainly affected by the mass loading is the electromechanical coupling coefficient k_t , which becomes k_{eff} when the electrodes are included [15]. The effective coupling coefficient k_{eff} can be calculated as the difference between the resonance and antiresonance frequency as [14],

$$k_{eff}^2 = \left(\frac{\pi^2}{4} \right) \left(\frac{f_r}{f_a} \right) \left(\frac{f_a - f_r}{f_a} \right) \quad (4)$$

The value of k_{eff} will depend on the electrode and piezoelectric characteristics, and there are two different ways to calculate it: solving the fundamental equations in a BAW resonator taking into account the symmetries in the structure [16], or using the definition of mechanical energy as in [17]. The final result is the variation of k_{eff} with the thickness ratio between the electrode and piezoelectric slab t_e/d_p . This variation can be found in Figure 3, where using Zinc Oxide as a piezoelectric material, four different curves are shown for a different metal electrodes material. Each of the four different curves shows an optimum ratio t_e/d_p where the achieved k_{eff} is maximum. This is usually a design rule of a BAW resonator: adjust the thickness of the electrode and piezoelectric slab to achieve the optimum k_{eff} . It is straightforward now to state that, for the present structure, $k_{eff_1} \neq k_{eff_2}$ since the ratio t_e/d_p in both cases is different. Then, taking the previous consideration into account, the full structure can be understood as two independent resonators electrically connected in shunt configuration which can be modeled as shown in Figure 4, where the subscript $x = 1$ refers to the central area of the resonator, which is the area confined between the thickened edge load, and $x = 2$ refers to the thickened edge load region. In this case, it can be advanced that a new resonating mode will be present in the electrical behavior of the

BAW resonator due to the thickened edge load. Each of the lumped elements considered in the equivalent circuit is defined as,

$$\begin{aligned}
 C_{0x} &= \frac{A_x \varepsilon_r \varepsilon_0}{d_p} \\
 C_x &= \frac{8C_{0x} k_{eff_x}^2}{\pi^2 - 8k_{eff_x}^2} \quad x = 1, 2 \\
 L_x &= \frac{\pi^2}{8k_{eff_x}^2 \omega_{ax}^2 C_{0x}}
 \end{aligned} \tag{5}$$

The set of equations in (5) shows that each BAW resonator is completely defined with $\omega_a = 2\pi f_a$, the antiresonance frequency that is directly related with the thickness, the effective coupling coefficient k_{eff} which depends on the mass loading effect, and the static capacitance C_0

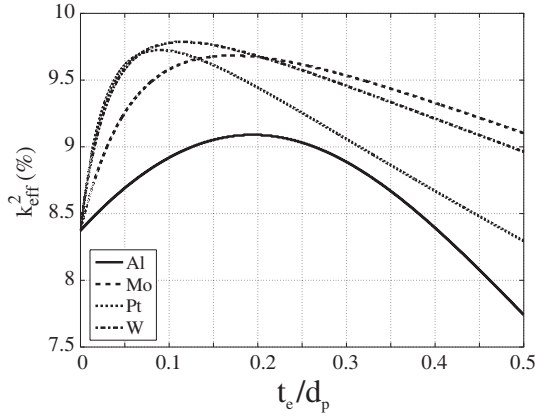


Figure 3. Effective electromechanical coupling constant as a function of the thickness ratio for Zinc Oxide Piezoelectric material.

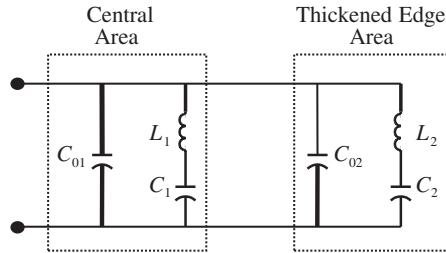


Figure 4. Equivalent electrical circuit for the thickened edge configuration using the Butterworth-Van Dyke equivalent.

of each resonator, being d_p the thickness of the piezoelectric slab. Then, the input electrical impedance from the proposed electric equivalent circuit in Figure 4 can be computed as,

$$Z(\omega) = \frac{(w^2 L_1 C_1 - 1)(w^2 L_2 C_2 - 1)}{w^4 (L_1 C_1 L_2 C_2 C_0) + w^2 (-C_0 (L_1 C_1 L_2 C_2) - C_1 C_2 (L_1 + L_2) + C_0 + C_1 + C_2)} \quad (6)$$

where $C_0 = C_{01} + C_{02}$. Analyzing (6), it can be seen that the magnitude of the electrical impedance is zero for,

$$\begin{aligned} \omega_{r1} &= 1/\sqrt{L_1 C_1} \\ \omega_{r2} &= 1/\sqrt{L_2 C_2} \end{aligned} \quad (7)$$

namely, each BAW resonator contributes with a resonance frequency f_r that only depends on the mechanical arm of each resonator. In the case of the antiresonance frequency f_a , the magnitude of the electrical impedance must be infinite. Solving the roots of the denominator, two antiresonance frequencies are given at,

$$\begin{aligned} \omega_{a1} &= \frac{1}{2A} \sqrt{-2A \left(B + \sqrt{B^2 - 4AC} \right)} \\ \omega_{a2} &= \frac{1}{2A} \sqrt{-2A \left(B - \sqrt{B^2 - 4AC} \right)} \end{aligned} \quad (8)$$

where, $A = L_1 C_1 L_2 C_2 C_0$, $B = -C_0 (L_1 C_1 + L_2 C_2) - C_1 C_2 (L_1 + L_2)$ and $C = C_0 + C_1 + C_2$ corresponding to the shunt equivalent capacitance of the equivalent model.

In Figure 5, the comparison between the proposed one-dimensional equivalent circuit and three-dimensional simulation by means of the finite element simulator ANSYS is shown in a wider frequency range. At 1.750 GHz, the first resonant mode is found, which is due to the thickened edge load. Moving to higher frequencies, the fundamental mode can be found at 1.9 GHz. The agreement between both responses is very good in terms of the allocation of the resonant frequencies and the value of the effective electromechanical coupling constant. However, as discussed, the one-dimensional equivalent cannot predict the lateral effects in the electrical behavior of the BAW resonator. In Figure 6(a), the mechanical displacement distribution for the mode due to the thickened edge load is shown. It can be seen that the distribution is confined in the thickened edge load region. In Figure 6(b), the mechanical displacement distribution is shown for the fundamental mode, where as can be seen, it is confined in the active area of the BAW resonator.

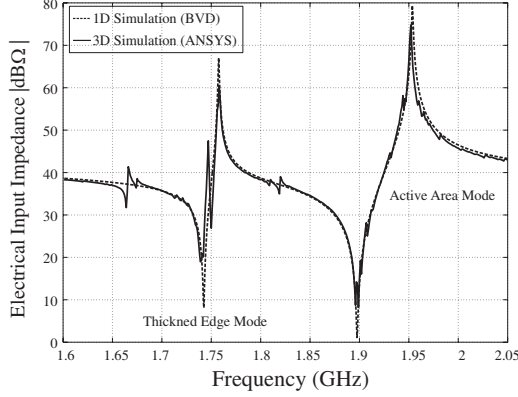


Figure 5. Electrical impedance using the one- (dashed line) and the three-dimensional simulation (solid line).

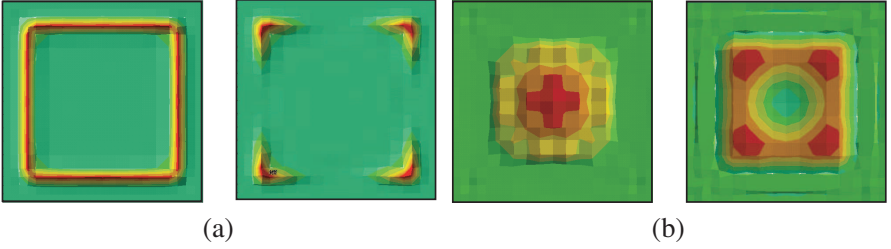


Figure 6. Mechanical distribution at the resonance (Right) and antiresonance (Left) frequency in the z -direction for each of the two resonant modes in Figure 5. (a) Corresponds to the mechanical displacement distribution of the mode due to the thickened edge load 1.750 GHz. The mechanical distribution is confined in the perimeter of the BAW resonator. (b) Corresponds to the mechanical displacement distribution of the main mode between at 1.9 GHz. In this case, the mechanical distribution is confined in the center area of the BAW resonator.

3.1. Effective Coupling Coefficient Degradation

It has been previously discussed that the thickened edge load contributes to a resonant mode placed at its own cut-off frequency, which depends on the used height h for the thickened edge load. In a first approach, each region has been considered as an independent BAW resonator. This is accomplished in terms of resonance frequency since w_{r1} and w_{r2} only depends on the mechanical arms of each BAW resonator. However, as can be seen in Figure 2(a), the

antiresonance frequency allocation has been shifted down with respect to the conventional case. As analyzed from the expression in (6), the value of the antiresonance not only depends on each of the lumped components associated to each resonator. When the area of the thickened edge load is big enough, as discussed, a resonant mode is present in the electrical behavior of the BAW resonator. In this case, part of the energy contained in the fundamental mode of the active area leaks to the surrounding region, making the effective electromechanical coupling constant k_{eff1} to be degraded. Since the frequency allocation of the resonance frequency is fixed by the motional arm, the antiresonance frequency allocation deviates to lower values. This degradation depends on the value of n in Equation (3), where as the value is increased, the area of the thickened edge load region is bigger, leading to more energy leaking from the fundamental mode. From the expression for the input electrical impedance in (6), to increase the value of n is directly related with the value of the static capacitance C_{02} since this is proportional to the area A . The lower value of n leads to a negligible value of C_{02} . In this case, the inductance L_2 behaves as an open-circuit leading to the full structure to behave as a resonator with $C_0 \simeq C_{01}$ and a motional arm composed by the L_1 - C_1 circuit. From the energetic point of view, since the area of the thickened edge load is almost negligible, a very little part of the energy of the fundamental mode leaks to the thickened edge load region mode, and thus, the antiresonance frequency is allocated at the expected position with no degradation of the effective electromechanical coupling constant.

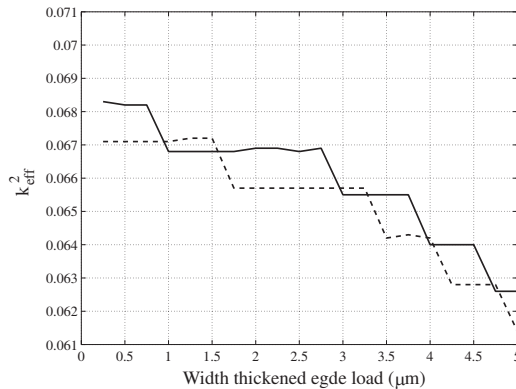


Figure 7. Measured effective electromechanical coupling constant as a function of the width W_2 of the group of resonators with $f_r = 1.907$ MHz (solid line) and $f_r = 1.963$ MHz (dashed line).

In order to validate these results, the effective electromechanical coupling constant of two different groups of BAW resonators has been measured. The first group is composed of resonators with $f_r = 1.907$ MHz, while the second group presents a resonance frequency of $f_r = 1.963$ MHz. In both groups, a thickened edge load was included where the value of the width was designed from $0.25\text{ }\mu\text{m}$ to $5\text{ }\mu\text{m}$ in steps of $0.25\text{ }\mu\text{m}$. The variation of the effective electromechanical coupling constant as a function of the width W_2 is shown in Figure 7. It can be clearly seen that as the width W_2 becomes greater, the value of the effective electromechanical coupling becomes degraded.

4. CONCLUSION

Before lateral unwanted resonances, the thickened edge load in the top electrode offers a very good performance in the electrical behavior of the BAW resonator. A brief discussion in the development of the set of expressions for the width of the thickened edge load has been done. The central area and also the thickened edge load area can be modeled by means of independent Butterworth-Van Dyke equivalents since the mass loading effect and propagation condition are different at each region. The proposed electric equivalent circuit predicts, on one hand, the presence of a mode due to the thickened edge load and on the other hand, the degradation of the effective electromechanical coupling constant due to the leaking of energy from the fundamental mode to the mode because of the thickened edge load. In order to validate this, the results of measured resonators have been shown.

REFERENCES

1. Lakin, K. M., G. R. Kline, and D. T. McCarron, "High-Q microwave acoustic resonators and filters," *IEEE Transactions on Microwave Theory and Techniques*, 2139–2146, 1993.
2. Shockley, W., C. R. Curran, and D. J. Koneval, "Energy trapping and related studies of multiple electrode filter crystals," *17th Annual Symposium on Frequency Control*, 88–126, 1963.
3. Curran, D. R. and D. J. Koneval, "Energy trapping and the design of single and multi-electrode filter crystals," *18th Annual Symposium on Frequency Control*, 93–119, 1964.
4. Mason, W. P., "Equivalent electromechanical representation of trapped energy transducers," *Proceedings of the IEEE*, Vol. 57, 1723–1734, 1969.
5. Bradley, P., J. D. Larson III, and R. C. Ruby, "Bulk acoustic wave

- resonator withy improved lateral mode supression,” No. 6215375, April 2001.
6. Ruby, R., J. Larson, C. Feng, and S. Fazzio, “The effect of perimeter geometry on FBAR resonator electrical performance,” *IEEE MTT-S International Microwave Symposium Digest*, 2005.
 7. Makkonen, T., A. Holappa, J. Ella, and M. Salomaa, “Finite element simulations of thin-film composite BAW resonators,” *IEEE Transactions on Ultrasonics, Ferroelectrics and Frequency Control*, 1241–1258, 2001.
 8. Rosen, D., J. Bjurstrom, and I. Katardjiev, “Suppression of spurious lateral modes in thickness-excited FBAR resonators,” *IEEE Transactions on Ultrasonics, Ferroelectrics and Frequency Control*, 1189–1192, July 2005.
 9. Kaitila, J., M. Ylilammi, and J. Ella, “Resonator structure and a filter comprising such a resonator structure,” US Patent, No. 6812619, 2001.
 10. Fattinger, G. C., S. Marksteiner, J. Kaitila, and R. Aigner, “Optimization of acoustic dispersion for high performance thin film BAW resonators,” *IEEE Ultrasonics Symposium*, 2005.
 11. Jiu-Horng, L., T. Kung-Yu, C. Chih-Wei, and S. Yu-Ching, “Optimization of frame-like film bulk acoustic resonators for suppression of spuious lateral modes using finite element method,” *IEEE Ultrasonics Symposium*, 2004.
 12. David, J. and N. Cheeke, *Ultrasonic Waves*, CRC Press LLC, 2002.
 13. Rosenbaum, J. F., *Bulk Acoustic Wave Theory and Devices*, Artech House, 1988.
 14. Larson III, J. D., P. D. Bradley, S. Wartenberg, and R. C. Ruby, “Modified butterworth-van dyke circuit for FBAR resonators and automated measurement system,” *IEEE Ultrasonics Symposium*, 863–868, 2000.
 15. Menendez, O., P. de Paco, E. Corrales, and J. Verdu, “Procedure for the design of a Ladder BAW filters taking electrodes into account,” *Progress In Electromagnetics Research Letters*, Vol. 7, 127–137, 2009.
 16. Chao, M.-C., Z. Wang, Z.-N. Huang, S.-Y. Pao, and C. C. Lam, “Accurate explicit formulae of the fundamental mode resonant frequencies for FBAR with thick electrodes,” *IEEE Frequency Control Symposium and PDA Exhibition*, 794–801, 2003.
 17. Kaitila, J., “Review of wave propagation in BAW thin film devices progress and prospects,” *IEEE Ultrasonic Symp.*, 120–129, 2007.